High-resolution electron microscopy investigation of metal–support interactions in Rh/TiO_2

S. Bernal, F. J. Botana, J. J. Calvino, C. López, J. A. Pérez-Omil and J. M. Rodríguez-Izquierdo
Departamento de Ciencia de los Materiales, Ingeniería Metalúrgica y Química Inorgánica, Facultad de Ciencias, Universidad de Cádiz, Apdo 40, Puerto Real, 11510 Cádiz, Spain

High-resolution electron microscopy (HREM), combined with digital image processing and computer simulation techniques, has been used to carry out a microstructural characterization of some Rh/TiO_2 catalysts reduced at 473, 773 or 823 K. A sample resulting from the reduction of the catalyst at 773 K, reoxidized with flowing O_2 at 673 K and finally reduced at 473 K was also investigated. In contrast to earlier literature reports, the HREM images recorded here suggest the existence of some definite structural relationships between both the rutile and anatase titania microcrystals and the rhodium particles grown on them. Though some micrographs have been interpreted in terms of slightly reduced Magneli phases, our HREM study suggests that the major microstructural feature of the high temperature (773 and 823 K) reduced samples is the formation of an amorphous reduced titania phase, associated with which metal decoration occurs. Some metal sintering is also observed. The reoxidation treatment, although inducing reversal of the decoration process leads to larger metal particles than those of the starting low-temperature reduced catalysts. Note, also, that twinned metal particles are more often observed in the catalyst resulting from the mild reduction of the reoxidized sample.

For the last decade, EM techniques and, more specifically, HREM have been used increasingly in catalyst characterization. Although this latter technique has not yet been fully exploited it is evident that it can be fruitfully applied to the microstructural investigation of numerous heterogeneous catalysts, including highly dispersed metals,[1–4] oxides used as both active phases and supports,[2,3] sulfides[2,5,6] or zeolites.[7,8]

Since Tauster *et al.*[9] reported for the first time on the so-called strong metal–support interaction (SMSI) effect, much work has been carried out to elucidate the nature of this phenomenon. Typically, the SMSI effect is associated with reducible oxide supports,[10–14] M/TiO_2 being by far the most extensively investigated catalytic system.[12–14]

It is quite obvious that an in-depth microstructural investigation of the catalysts is critically important to arrive at a better interpretation of the SMSI effect. However, the number of EM studies devoted specifically to investigation of the SMSI effect are rather limited, even for titania-supported metal catalysts, the paradigmatic example of an SMSI system.

Transmission electron microscopy (TEM) was used in Tauster's work[9] to establish the metal particle size distribution in several M/TiO_2 catalysts. The information contained in TEM micrographs provided essential experimental support for one of the most characteristic features of the SMSI effect: the strong perturbation of the metal chemisorptive properties.[12,13,15] Baker *et al.*'s studies on Pt/TiO_2[16,17] can also be considered as pioneering contributions of EM to the investigation of the SMSI effect. By using TEM and selected area electron diffraction (SAED) patterns, they made some proposals about the microstructural nature of these catalysts which have been accepted for a long time. Thus, the analysis of the contrasts exhibited by the metal in Pt/TiO_2 catalysts allowed them to propose that, under the SMSI state, platinum forms flat pill-box shaped particles. Upon reoxidation,[17] the metal particles would recover their original hemispherical shapes. It was concluded that, inherent to the SMSI effect, the metal would spread over the support, this morphological change being considered as a characteristic feature of Pt/TiO_2 in SMSI state. Likewise, from an SAED pattern recorded for the catalysts reduced at 1075 K, the authors were able to identify the Ti_4O_7 phase. The formation of such a reduced phase was confirmed by the presence, in the Pt/TiO_2 catalysts reduced at 825 K, of some lattice spacings larger than those corresponding to the dioxide phases.[16] From these two observations, a relationship was established between the SMSI effect and the occurrence of a reduced titania phase, quite often formulated as Ti_4O_7.[11,16,18] These EM studies on Pt/TiO_2 were further extended by Baker *et al.* to several other metals such as Ag,[19] Ni,[20–22] Fe[23] and Pd.[24] TEM has also been applied to the investigation of titania-supported rhodium catalysts.[25–28]

In some of the studies mentioned above[20–22,24] support migration onto the metal particles was considered to be an important factor in characterizing the SMSI effect. However, the major experimental evidence for such a proposal actually came from a variety of spectroscopic studies.[21,29–35] It was necessary to use surface profile high-resolution imaging techniques[36] to obtain the very first EM evidence of metal decoration effects.[37–39] In ref. 38, however, the HREM image showing the covered rhodium particles corresponded to a Rh/TiO_2 catalyst reduced at very high temperature: 1073 K. Later,[38–40] HREM images of decorated metal particles were also obtained for Rh/TiO_2 catalysts reduced at 773 K, the temperature normally used to induce the SMSI state. HREM has also been applied to the investigation of Pt/TiO_2[41,42] and, more recently, Ru/TiO_2[43] catalysts. In the case of Ru/TiO_2 the authors indicated the presence of surface decoration effects while for the Pt/TiO_2 system, by combining experimental and computer-simulated images the authors in ref. 41 suggested that, in addition to metal decoration, Pt–Ti alloys are formed upon reduction at 773 and 973 K.

Our laboratory has been working on the chemical and microstructural properties of rare-earth-metal oxide-supported metal catalysts for some time.[4,40,44–56] Most of this work has dealt with Rh/4f oxide catalysts since, in accordance with the literature,[57,58] M/CeO_2 and even M/Ln_2O_3 can exhibit SMSI phenomena, the elucidation of the actual nature of such an effect in M/4f oxide catalysts has constituted a major objective of this investigation, in which HREM has been applied systematically.[4,40,44,51–54] In our project, the Rh/TiO_2 system was used as a reference catalyst exhibiting the SMSI effect. Here, we report an HREM study carried out on Rh/TiO_2. As will be discussed below, in spite of being considered a classic SMSI system, there are some aspects of its HREM characterization that were not sufficiently stressed in the earlier literature.

Experimental

The starting titanium dioxide was the sample P-25, from Degussa. To stabilize its textural and structural properties, the titania sample was heated in a flow of H_2 for 3 h at 773 K and then reoxidized for 4 h, at 673 K. The sample resulting from this pretreatment, with a surface area of 20 m^2 g^{-1}, consisted of a mixture of rutile (80%) and anatase (20%).

The Rh/TiO_2 catalysts were prepared by the incipient wetness impregnation technique from an aqueous solution of $Rh(NO_3)_3$. After the impregnation treatment, the sample was dried in air at 383 K, for 10 h and stored in a dessicator until its reduction. This impregnation–drying cycle was repeated several times to give a final metal loading of 5.0 wt.%.

The reduction treatments were carried out by heating the $Rh(NO_3)_3/TiO_2$ precursor system in a flow of H_2 (60 cm^3 min^{-1}) at 10 K min^{-1} from 298 K to the selected reduction temperature (473, 773 or 823 K). The samples were held for 1 h at the reduction temperature, then treated in flowing helium (60 cm^3 min^{-1}) for 1 h at the reduction temperature and, finally, they were cooled, also in a flow of inert gas. In the particular case of the catalysts reduced at 473 K, the sample was further heated in a flow of helium to 773 K. In this way, we ensure the elimination of the hydrogen chemisorbed on the catalysts, before its exposure to air. To prevent the fast reoxidation of the reduced catalysts, they were cooled to 191 K, always in a flow of helium, then treated with O_2 (5%)–He for 0.5 h, warmed to 295 K in the oxidizing mixture and finally exposed to the air. The samples prepared in this way were transferred into the microscope following the procedure reported elsewhere.[51]

The HREM images were obtained in a JEOL-2000 EX microscope with 0.21 nm point resolution. The instrument was equipped with a top-entry specimen holder and an ion pump. The computer simulated HREM images were obtained by running the EMS Software package on an IRIS 4D35/TG+ Silicon Graphics workstation. Digital processing of both calculated and experimental HREM images was performed with the help of the Semper 6+ software. Two computer programs, written in Fortran 77 and developed at the University of Cádiz, have also been routinely used in this work. The so called EJEZ program was designed to establish the set of zone axes of a known structure allowing one to obtain HREM images on a microscope of given structural resolution. The RHODIUS program has allowed us to build the complex supercell structural models used as the basis for the computer simulations presented in this work.

Results and Discussion

HREM has been used to characterize a series of Rh/TiO_2 catalysts prepared as described above. The lowest reduction temperature applied here, 473 K, is considered to lead to catalysts exhibiting conventional chemical behaviour.[13] The other two reduction temperatures, 773 and 823 K, however, would induce the onset of the SMSI state.[13] We have also studied the sample resulting from the reoxidation at 673 K and further re-reduction at 473 K, of the catalysts previously reduced at 773 K. This latter treatment is considered to allow the recovery of the catalysts from the SMSI state.[59] Hydrogen chemisorption data and catalytic activity measurements for the benzene hydrogenation reaction clearly indicate classical SMSI behaviour for the Rh/TiO_2 catalysts studied here.

HREM study of the Rh/TiO_2 catalysts reduced at 473 K

Fig. 1 shows a low-magnification general view of our low-temperature reduced Rh/TiO_2 catalysts. Note the high density of metal particles; in spite of this, the particle size distribution is quite narrow, Fig. 2(*a*), the mean size being *ca.* 3 nm.

Fig. 3(*a*) and (*b*) show two representative profile-view HREM images of the catalyst reduced at 473 K. They account, respectively, for anatase and rutile supported rhodium systems. In effect, by running the EJEZ program, we have established the zone axis along which high-resolution images of both anatase and rutile phases can be obtained in our microscope. The results from this study are summarized in Table 1.

In accordance with the crystallographic data included in Table 1, the HREM images in Fig. 3(*a*) and (*b*), as well as the corresponding diffraction patterns computed by digital processing techniques which are also included as an inset in the figure, can be interpreted as due to anatase close to [111] orientation and rutile in [001] orientation, respectively. The coexistence of Rh/TiO_2 (A) and Rh/TiO_2 (R) might well be expected if it is recalled that our titania support actually consists of a mixture of anatase (20%) and rutile (80%).

Regarding the supported rhodium phase, Fig. 3(*a*) and (*b*) confirm the high density of metal particles sitting on the support surface. The metal particles consist mainly of clean, well faceted single crystals oriented close to the [110] zone axis, the only one allowing us to obtain high-resolution rhodium images in our microscope.[4] Lattice fringes corresponding to Rh {111} planes at 0.220 nm can be easily resolved in Fig. 3(*a*) and (*b*). From a morphological point of view, the particles generally consist of truncated cuboctahedron crystals with external surfaces made up of {111} and {002} planes. Fig. 4 shows in perspective, as well as in [110] projection, the two types of more often observed metal crystallites.

The analysis of the images in Fig. 3 also suggests the existence of orientation relationships between the metal and the support. Thus, in the case of Fig. 3(*a*), *ca.* 80% of the metal particles have grown with their (002) faces parallel to the support surface. Likewise, Fig. 5 shows an HREM image of anatase in orientation close to [111]. Again, the (002) face of the metal particle is parallel to the support surface. In this figure, it can also be easily observed that, as a result of the orientation relationship, Rh (111) planes grow parallel to the (112) planes of anatase. The lattice spacings corresponding to the planes mentioned above are 0.220 nm for Rh (111) and 0.233 nm for TiO_2-A (112). These structural agreements suggest the existence of an epitaxial growth of the metal crystallites on the support.

In the case of the rutile-supported rhodium system, Fig. 6 also suggests the existence of defined structural relationships. The image in Fig. 6 corresponds to the catalysts reduced at

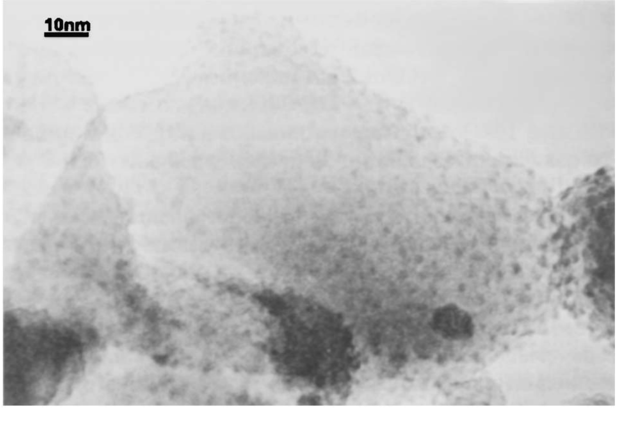

Fig. 1 Low-magnification image of the Rh/TiO_2 catalyst reduced at 473 K

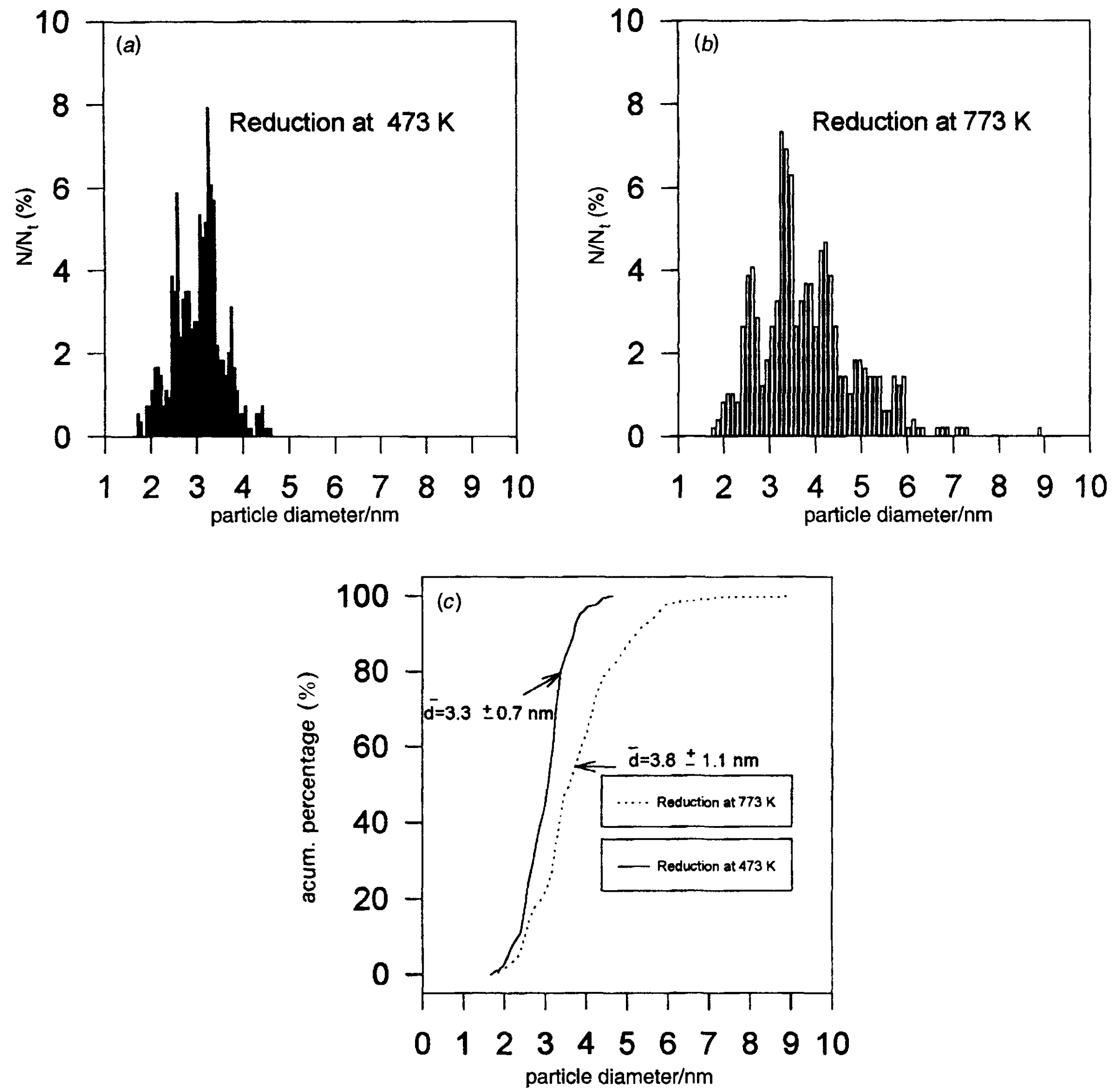

Fig. 2 Particle size distributions obtained from the analysis of HREM images of the Rh/TiO$_2$ samples reduced at (*a*) 473 and (*b*) 773 K. (*c*) Integrated size distribution curves for the above-mentioned reduction temperatures.

773 K, further oxidized at 673 K and finally re-reduced at 473 K. Although some additional aspects of this catalyst sample will be discussed below, here, we shall focus our attention on the metal–support structural relationship. In effect, the HREM image in Fig. 6(a) shows a rhodium crystallite in [110] orientation and based on a (002) plane, sitting on a [101] plane of rutile in [010] orientation. This implies that Rh {111} planes (lattice spacing 0.220 nm) grow nearly parallel to TiO$_2$-R {103} planes (lattice spacing 0.243 nm).

Fig. 6(c) and (d), which were constructed by running the RHODIUS program developed at UCA, show schematic drawings depicting the crystallographic details of this relationship. The calculated HREM image, Fig. 6(b), obtained from the structural model in Fig. 6(c) shows a very good match with the experimental image, Fig. 6(a), thus confirming our proposal. As suggested in Fig. 7(a), the epitaxial relationship established between the metal and support planes contacting at the interface could be responsible for the observed orientation effects. According to this figure, a good structural correspondence is attained allowing us to define a small-size coincidence cell that can be repeated periodically along the [110] and [1-10] Rh directions. As marked in Fig. 7, the dimensions of this coincidence cell are 2.5 [110] Rh × 1 [1-10] Rh.

The above orientation relationships can be considered representative of the set of micrographs analysed in this work, but we cannot rule out the existence of some others. We have carried out a comparative analysis of the crystallography of anatase and rhodium planes by using the EJEZ program. From this analysis an epitaxial growth of Rh (002) on TiO$_2$ (001) should be expected because it is also possible to define, as observed in Fig. 7(b), a very small and periodic coincidence lattice. The orientation relationship associated with this epitaxial growth could be defined as follows, Rh [100]‖TiO$_2$ [100], Rh (001)‖TiO$_2$ (001). To confirm this idea experimentally it would be necessary, according to data included in Table 1(b), to analyse micrographs of Rh on TiO$_2$-A showing a support in {100} or {110} orientations and with extended flat (001) surfaces. However, this information was not available from our HREM images.

The observation of orientation relationships between rhodium and both anatase and rutile support phases contrasts with that reported by Singh *et al.*[37] They proposed that rhodium does not exhibit preferred orientations relative to TiO$_2$. It should be mentioned, however, that this latter conclusion was based on the observation of continuous diffraction rings in the corresponding electron diffraction patterns. This experimental basis has some drawbacks. First, in the case of powder polycrystalline catalysts, the identification of preferential orientations from electron diffraction patterns may require the use of a conventional SAED technique with a narrow electron probe or even better nanodiffraction tech-

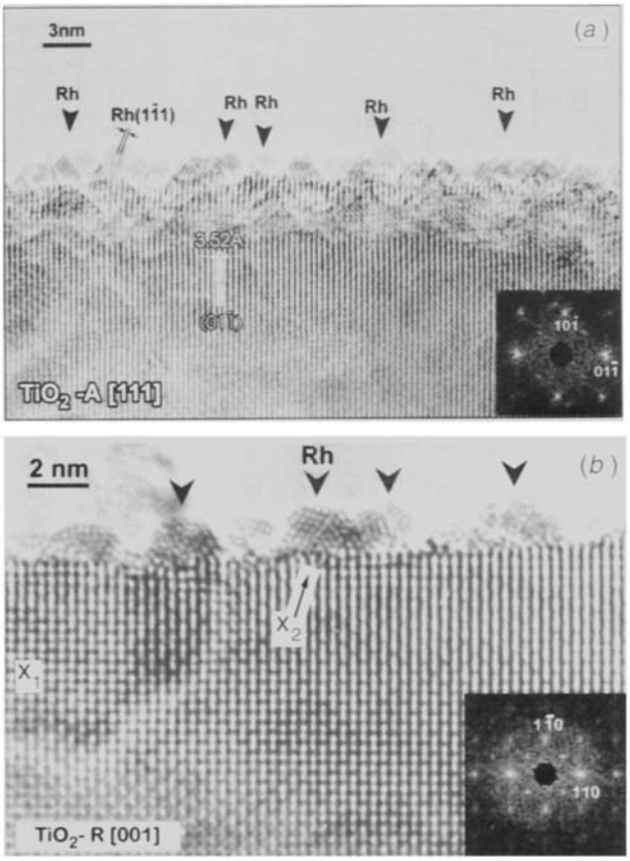

Fig. 3 HREM profile-view images of the catalyst reduced at 473 K, showing rhodium particles sitting on (*a*) anatase close to [111] orientation and (*b*) rutile in [001] orientation

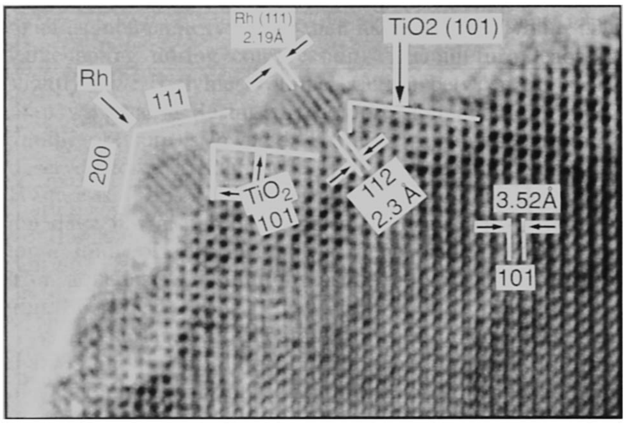

Fig. 5 HREM view of the catalyst reduced at 473 K. Note the parallel alignment between the (111) planes of rhodium and the (112) planes of anatase.

niques.[60] Otherwise, many randomly oriented catalyst particles can contribute to the diffraction process, thus leading to ring patterns, with independence of the structural relationships existing between metal and support. Secondly, because of the closeness of support and metal lattice spacings, 0.233 nm for TiO_2-A {1-12} or 0.219 nm for TiO_2-R {1-11} and 0.220 nm for Rh {111}, it is difficult to resolve the diffraction spots due to rhodium from those generated by the support lattice.

The HREM study of Rh/TiO_2 reduced at 473 K has also provided some useful information about the support reduction state. Fig. 8 shows support images which could be observed in some limited regions of the series of micrographs recorded for this catalyst. The contrasts observed in Fig. 8(a),

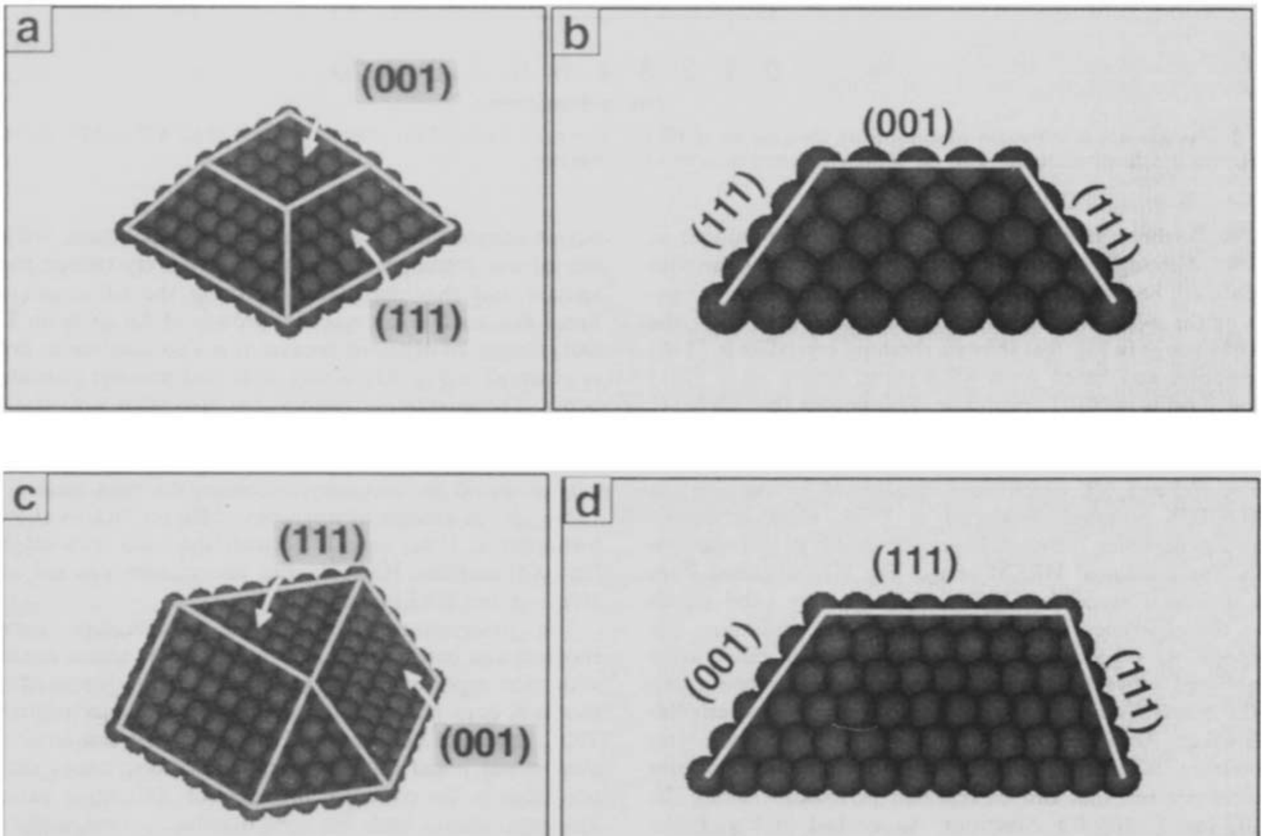

Fig. 4 Perspective view of truncated cuboctahedrons with (a) hexagonal and square faces and (c) triangular and square faces. The same models in [110] projection are shown in (b) and (d), respectively.

Table 1 Lattice spacings and angles for TiO_2-R and TiO_2-A in different orientations

zone axis	$(hkl)_1$	$(hkl)_2$	d_1 /nm	d_2 /nm	angle d_1d_2/degrees
(*a*) TiO_2 rutile					
001	0 1 0	1 0 0	0.459	0.459	90.0
	1 1 0	1 0 0	0.325	0.459	45.0
	1 −1 0	1 0 0	0.325	0.325	90.0
	2 0 0	0 1 0	0.230	0.459	90.0
	2 0 0	1 1 0	0.230	0.325	45.0
	0 2 0	2 0 0	0.230	0.230	90.0
010	0 0 1	1 0 0	0.296	0.459	90.0
	1 0 1	1 0 0	0.249	0.459	57.2
	1 0 1	0 0 1	0.249	0.296	32.8
	1 0 −1	1 0 1	0.249	0.249	65.6
	2 0 0	0 0 1	0.230	0.296	90.0
	2 0 0	1 0 1	0.230	0.249	57.2
110	0 0 1	1 −1 0	0.296	0.325	90.0
	1 −1 1	1 −1 0	0.219	0.325	47.7
	1 −1 1	0 0 1	0.219	0.296	42.3
	−1 1 1	1 −1 1	0.219	0.219	84.6
011	0 1 −1	1 0 0	0.249	0.459	90.0
	2 0 0	0 1 −1	0.230	0.249	90.0
	1 1 −1	1 0 0	0.219	0.459	61.6
	1 1 −1	0 1 −1	0.219	0.249	28.4
	1 1 −1	2 0 0	0.219	0.230	61.6
	1 −1 1	1 1 −1	0.219	0.219	56.9
111	1 0 −1	1 −1 0	0.249	0.325	67.5
	0 1 −1	1 0 −1	0.249	0.249	45.0
112	1 1 −1	1 −1 0	0.219	0.325	90.0
121	1 −1 1	1 0 −1	0.219	0.249	68.7
(*b*) TiO_2 anatase					
010	1 0 1	0 0 2	0.352	0.476	68.3
	1 0 −1	1 0 1	0.352	0.352	43.4
	1 0 3	0 0 2	0.243	0.476	40.0
	1 0 3	1 0 1	0.243	0.352	28.4
	1 0 3	1 0 −1	0.243	0.352	71.7
	1 0 −3	1 0 3	0.243	0.243	80.0
	0 0 4	1 0 1	0.238	0.352	68.3
	0 0 4	1 0 3	0.238	0.243	40.0
111	0 1 −1	1 0 −1	0.352	0.352	82.2
	1 −1 0	1 0 −1	0.268	0.352	49.0
	1 1 −2	1 0 −1	0.233	0.352	41.1
	1 1 −2	1 −1 0	0.233	0.268	90.0
110	1 −1 0	0 0 2	0.268	0.476	90.0
	0 0 4	1 −1 0	0.238	0.268	90.0
	1 −1 2	0 0 2	0.233	0.476	60.6
	1 −1 2	1 −1 0	0.233	0.268	29.4
	1 −1 2	0 0 4	0.233	0.238	60.6
	−1 1 2	1 −1 2	0.233	0.233	58.7
001	1 −1 0	1 1 0	0.268	0.268	90.0
131	0 1 −3	1 0 −1	0.243	0.352	73.5
	1 −1 2	1 0 −1	0.233	0.352	67.0
	1 −1 2	0 1 −3	0.233	0.243	39.5
331	1 0 −3	1 −1 0	0.243	0.268	63.0
	0 1 −3	1 0 −3	0.243	0.243	54.0
351	1 −1 2	1 0 −3	0.233	0.243	88.9
021	1 −1 2	1 1 −2	0.233	0.233	76.1

which cannot be interpreted in terms of any of the TiO_2 polymorphs, suggest the presence of phases belonging to the Magneli series Ti_nO_{2n-1}, in our catalyst. The above-mentioned contrasts can be considered as a characteristic feature of phases exhibiting crystallographic shear (CS),[61] thus supporting the later proposal. As is well known, Magneli phases result from the annihilation of oxygen vacancies through a CS mechanism.[62]

To confirm this tentative interpretation, we have carried out a computer simulation of the HREM image corresponding to a slightly reduced member of the Magneli series containing CS on the {132} planes. Displacement vectors along the $\frac{1}{2}$[0-11] TiO_2-R direction and a distance equivalent to 9 {132} planes between the CS-planes have been considered, Fig. 8(c). These structural details correspond to a local composition close to Ti_9O_{17} ($TiO_{1.889}$). The structural model was built up with the help of the RHODIUS program developed by us. The simulation conditions were the following: sample thickness 3 nm, electron beam accelerating voltage 200 kV, objective lense aperture diameter 12 nm^{-1}, defocus 50 nm, Cs 0.7

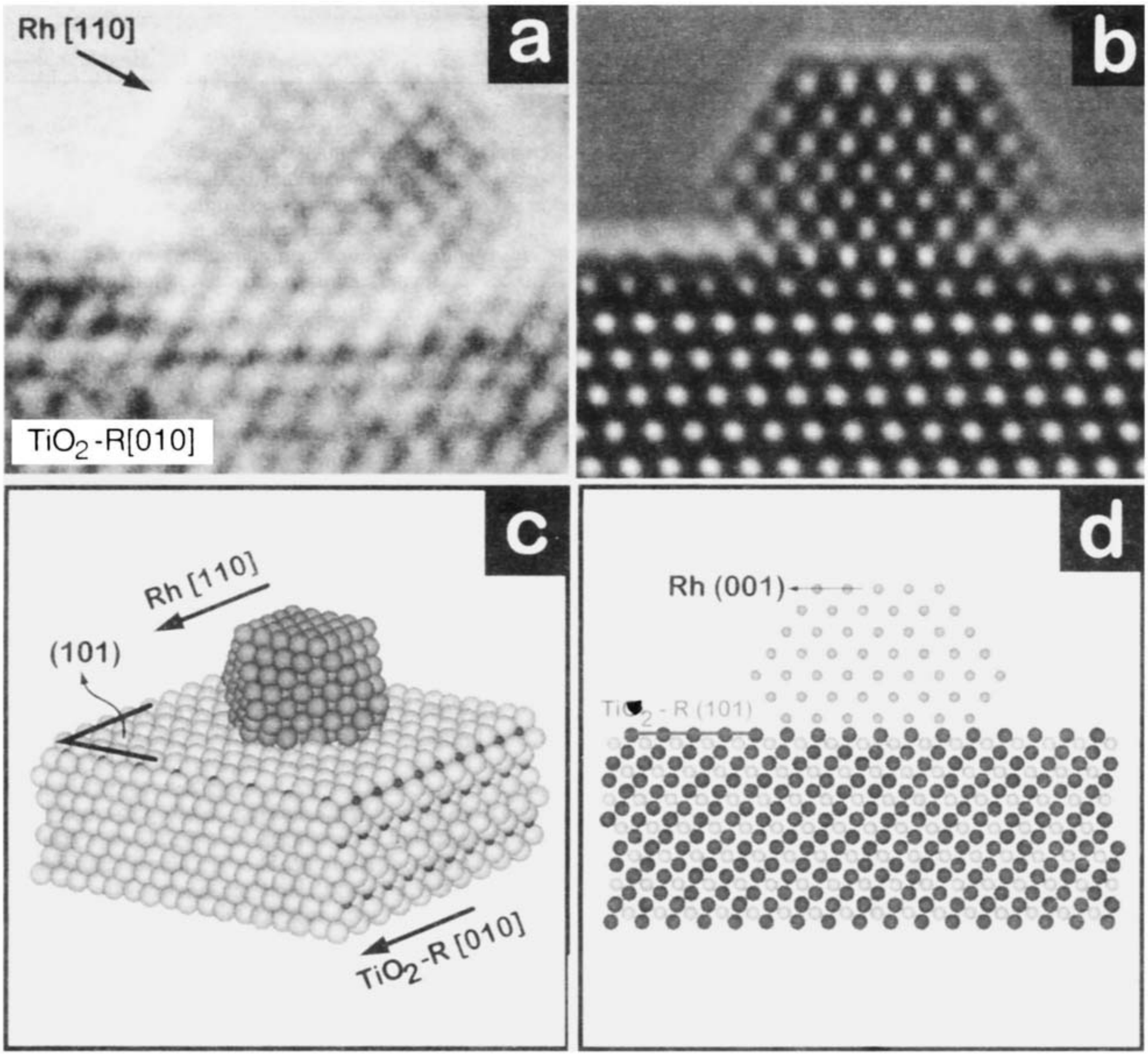

Fig. 6 Epitaxial growth of a rhodium particle on rutile. (a) HREM experimental image, (b) simulated image, (c) perspective view of the structural model built using the RHODIUS program to obtain the simulated image, (d) the same model shown in [110]-Rh projection.

mm, beam semiconvergence 1.5 mrad, defocus spread 10 nm. Upon comparison of both computed, Fig. 8(b), and experimental images, Fig. 8(c), we conclude the existence of a good fit between them. This confirms the presence in our catalyst reduced at 473 K of small regions which can be described in terms of very slightly reduced Magneli phases.

To exclude the likely possibility of formation of this reduced phase under the electron beam, a region of our unreduced precursor/support system $Rh(NO_3)_3/TiO_2$ was heavily irradiated for a period of time much longer than that usually spent in ordinary HREM studies. The growth of Magneli phases could not be observed.

Several authors have reported that, in the presence of rhodium, titania reduction can occur at relatively mild temperatures.[25,26,35] In ref. 35 this conclusion was drawn from a study on model Rh (Pt)/TiO_2 systems carried out with the help of surface analysis techniques such as Auger electron spectroscopy (AES), secondary ion mass spectroscopy (SIMS) and thermal desorption spectroscopy (TDS). Likewise, Yacamán,[26] by analysing the TEM contrasts observed in the support regions surrounding the rhodium particles, has also suggested the occurrence of local reduction of titania in an Rh/TiO_2 catalyst treated with H_2 at 573 K. The temperature-programmed reduction (TPR) study reported in ref. 25 would be consistent with the occurrence of some titania reduction at temperatures well below 773 K. This is also true in our case. Fig. 9 shows the TPR study carried out on the sample investigated here. As already noted by Prins and co-workers,[25] for well dispersed titania-supported rhodium catalyst, metal reduction takes place at fairly low temperatures, even at 295 K. Fast rhodium reduction, at 298 K, has also been observed on Rh/CeO_2.[55] The results reported in Fig. 9(a) would also be in agreement with that, the hydrogen consumption at room temperature: 1.19 (mmol H_2) g^{-1}, being higher than that required to reduce thoroughly the rhodium precursor to the metallic state: 0.68 (mmol H_2) g^{-1}. As deduced from both the strong H_2 consumption peak at 473 K, in Fig. 9(b), and the absence of further hydrogen uptakes at higher temperatures, the incorporation of hydrogen to the support would occur at 473 K or below. Though this does not necessarily mean that oxygen vacancies are created at such a low temperature,[54,63] it would not be excluded that part of the chemisorbed H_2 can lead to H_2O formation under these mild conditions. In fact, the reduced regions observed in Fig. 8 represent a minor fraction of the whole support.

To our knowledge, the presence of Magneli phases on M/TiO_2 catalysts reduced at such a low temperature has not been reported previously. Moreover, except for the TEM–

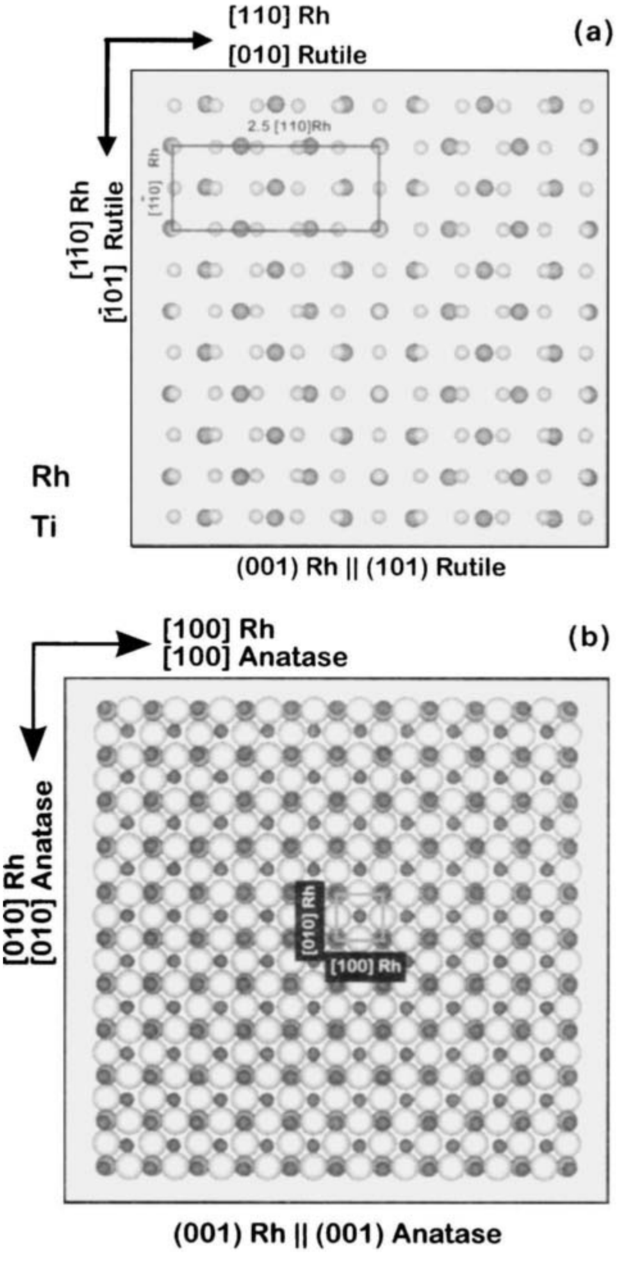

Fig. 7 Structural model of metal/support interfaces made up of (a) an (001) Rh plane on a (101) plane of rutile, and (b) an (001) Rh plane on (001) anatase. In both cases the corresponding periodic coincidence cells, and their dimensions, have been marked.

SAED studies by Baker *et al.*,[16,17] which were carried out on catalysts reduced at temperatures well above those normally used to induce the SMSI effect, no evidence of crystalline reduced phases of titania has been obtained from TEM/HREM. In fact, the HREM studies carried out on catalysts reduced at 773 K,[38,39] and even higher reduction temperatures,[37] did not find any indication of the presence of such phases.

HREM study of the Rh/TiO$_2$ catalyst reduced at high temperature (773 and 823 K)

Fig. 10 shows an HREM image of our Rh/TiO$_2$ catalyst reduced at 773 K. There are a number of aspects worth commenting on in relation to this figure. First, the occurrence of metal decoration effects can be clearly observed. As already reported in ref. 37–39, the amorphous layer covering the rhodium crystallite is a few Å thick. As deduced from Fig. 11–13, this covering effect is partial, in spite of the fact that the amount of H$_2$ chemisorbed by our catalyst is negligible.[40] This observation would be in agreement with the suggestion made by Sanz and co-workers[14] in the sense that the SMSI effect actually consists of a combination of both electronic and geometric effects.

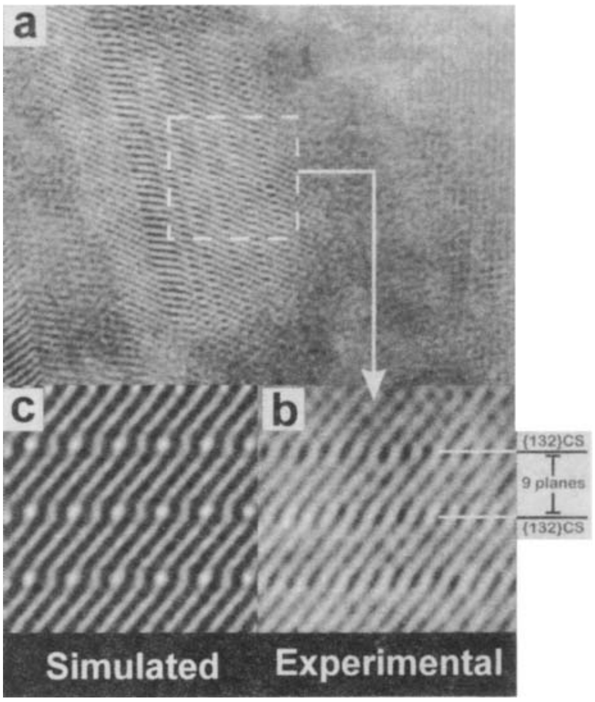

Fig. 8 HREM images of the Rh/TiO$_2$ catalysts reduced at 473 K showing the growth of Magneli phases in a small region: (a) general view, (b) enlargement of the squared region in (a) and (c) simulated image of a member of the Magneli phases containing CS defects on one of each nine {132} planes

The profile-view HREM image in Fig. 10 clearly indicates that the outer support layers actually consist of a thin amorphous phase covering the whole support. No increases in the number or size of crystalline patches like those shown in Fig. 8 could be observed. The same is true for the catalyst reduced at 823 K. In contrast, for this latter catalyst the support amorphization becomes much heavier, Fig. 11, and, correspondingly, there is an increase in the fraction of decorated/fully covered metal particles. Nevertheless, as deduced from Fig. 11 and 12, part of the metal surface is still free from support.

To rule out the possibility that the contrasts observed on the surface of the metal particle in Fig. 12 were due to an incomplete growth of a {111} plane at the surface, a digital intensity profile was recorded along the [111] direction inside the region marked with an A, Fig. 12(b). In this profile, an interplanar spacing of 0.30 nm is clearly identified. This value, which is rather large in comparison with the 0.220 nm spacing characteristic of Rh {111} planes, confirms that this image can be interpreted in terms of a metal particle partially decorated by support.

All the HREM studies on Rh/TiO$_2$ reduced at 773 K or above[37–39] have agreed on the presence of an amorphous surface phase in the support. In fact, it is explicitly stated in ref. 37–39 that they were unable to identify crystalline reduced phases of titania. Therefore, it seems to be very likely that the formation of the reduced amorphous phase, rather than the ordering of the oxygen vacancies in Magneli phases, constitutes a key feature for the onset of the metal decoration effects.

Our HREM study of the Rh/TiO$_2$ catalysts reduced at 773 K, and even 823 K, have not provided any evidence for dramatic morphological changes in the metal, such as those leading to raft-like particles as a result of their spreading over the support. This type of effect was reported earlier for Pt/TiO$_2$ [16,17] and for Rh/TiO$_2$.[37] Our observation would be

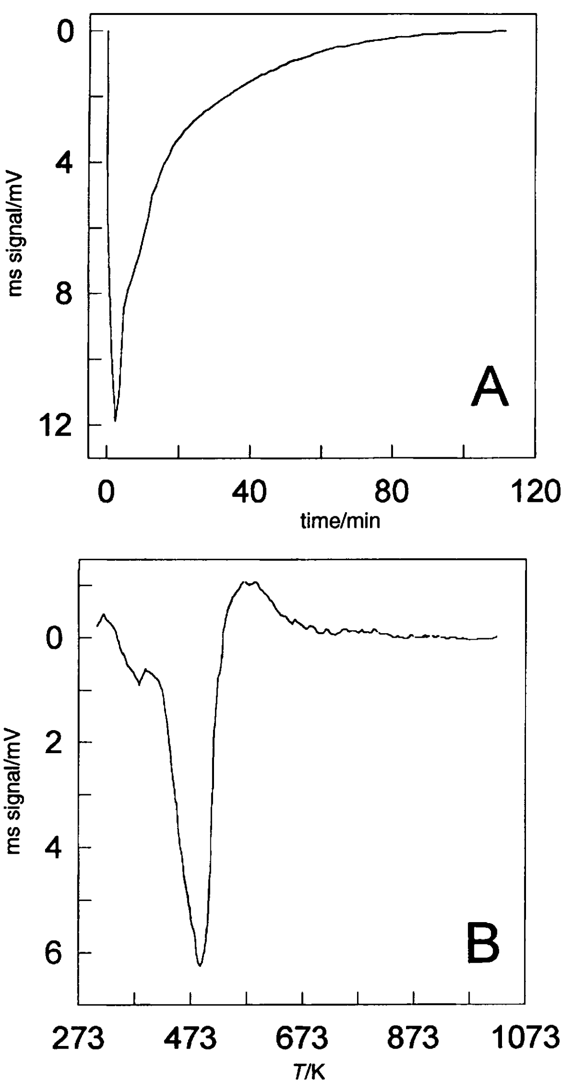

Fig. 9 TPR study of the Rh/TiO$_2$ catalysts: hydrogen consumption (a) at room temperature and (b) during the heating treatment, at a rate of 10 K min^{-1}

in agreement with the suggestion made in the review work on the SMSI effect by Tauster,[12] that, from a more detailed analysis of the literature, no morphology change takes place in the case of Rh/TiO$_2$ catalysts. We may note, however, a significant increase in the metal particle size. According to Fig. 2(*b*), the sample reduced at 773 K contains metal particles

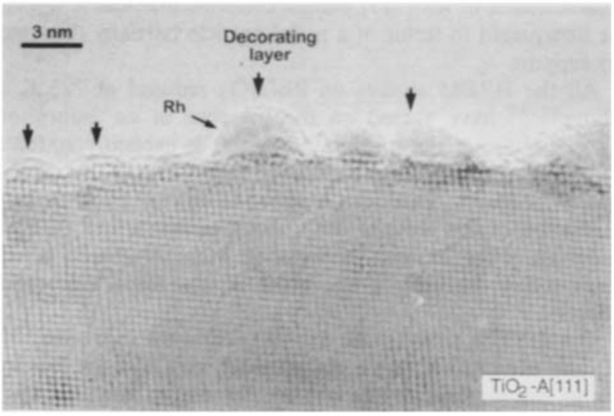

Fig. 10 HREM image of the catalysts reduced at 773 K. Note the growth of a thin amorphous layer on the metal particles and the support.

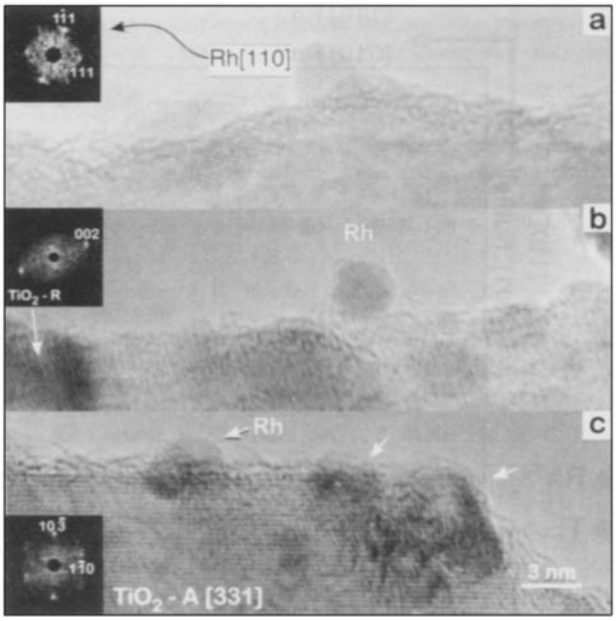

Fig. 11 HREM images recorded on different regions of the catalyst, reduced at 823 K, showing decoration effects

In parallel with this shift, the mean particle size increased from 3.3 ± 0.7 to 3.8 ± 1.1 nm. This implies that, associated with the high-temperature reduction treatment there is some rhodium sintering. This effect would probably allow us to explain the significant increase in the number of twinned particles observed upon increasing the reduction temperature

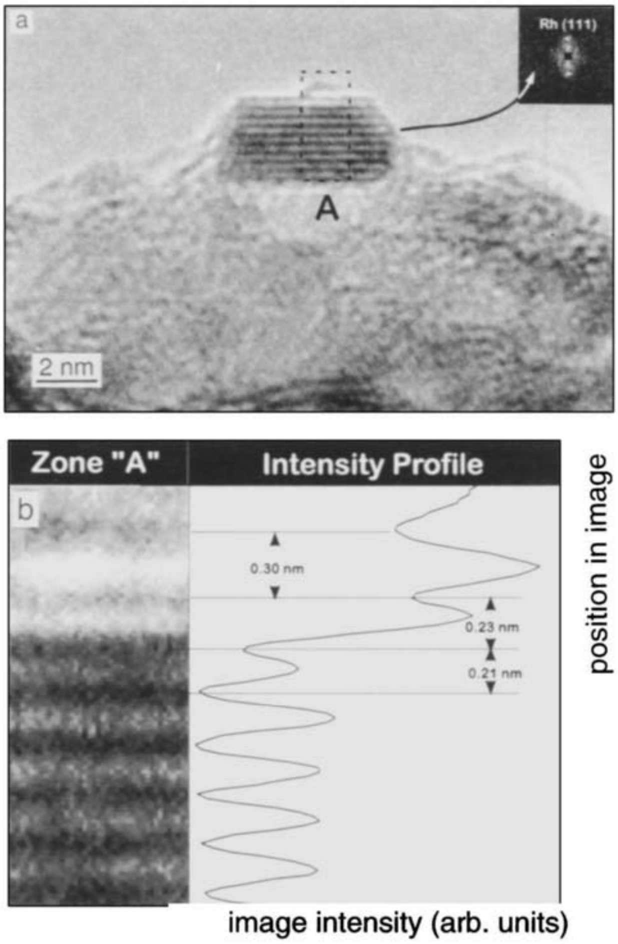

Fig. 12 (a) HREM image of the catalyst, reduced at 823 K, showing a partial coverage effect, (b) enlargement of the region marked as A and its corresponding digital intensity profile recorded along the [111]-Rh direction

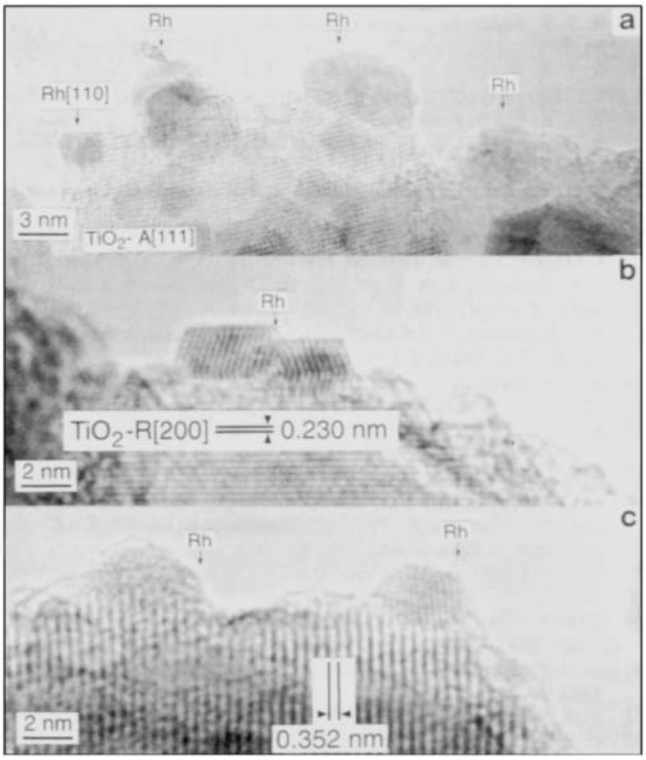

Fig. 13 HREM images of the catalyst reduced at 823 K clearly showing the existence of metal particles with clean surfaces

from 473 to 773 or 823 K, Fig. 13(a). These findings contrast with the absence of significant metal sintering reported in ref. 37 for Rh/TiO_2 catalysts reduced at even higher temperatures.

HREM study of the reoxidation effects on a Rh/TiO_2 catalyst reduced at high temperature

In accordance with the procedure normally followed to recover the Rh/TiO_2 catalysts from the SMSI state,[59] a sample reduced at 773 K was further reoxidized with flowing O_2 at 673 K, for 1 h, and re-reduced at low temperature, 473 K. Fig. 14 shows HREM micrographs recorded for this catalyst. They correspond to rhodium particles in orientation close to [110] sitting on rutile oriented along the [010] direction. Most of the metal particles look to be clean and well faceted, thus indicating the reversion of the decoration effect. The recovery from the SMSI state is not complete. Thus, we have found that some regions of the support surface and a small fraction of the metal particles [encircled particle in Fig. 14(a)] still demonstrate decoration effects. Likewise, on some micrographs of this catalyst, Fig. 15(a), we may note the presence of small regions where large lattice fringe spacings characteristic of Magneli phases are still present. These two observations suggest that the reoxidation treatment at 673 K does not guarantee a complete recovery of a fully unreduced support. A rather similar observation has also been reported in ref. 39. However, the results above were obtained after a prolonged treatment, overnight, under milder reoxidation conditions: 573 K and 200 Torr of O_2.

The HREM images in Fig. 15 also raise the question as to whether the reduced phase which was reported to occur on the sample reduced at 473 K, was actually formed upon low-temperature reduction, in the presence of rhodium or was already present in the pretreated support as a consequence of an incomplete reoxidation of the titanium dioxide. With independence of its origin, it seems, as already discussed, that this type of phase does not play an important role in determining the onset of the SMSI effect.

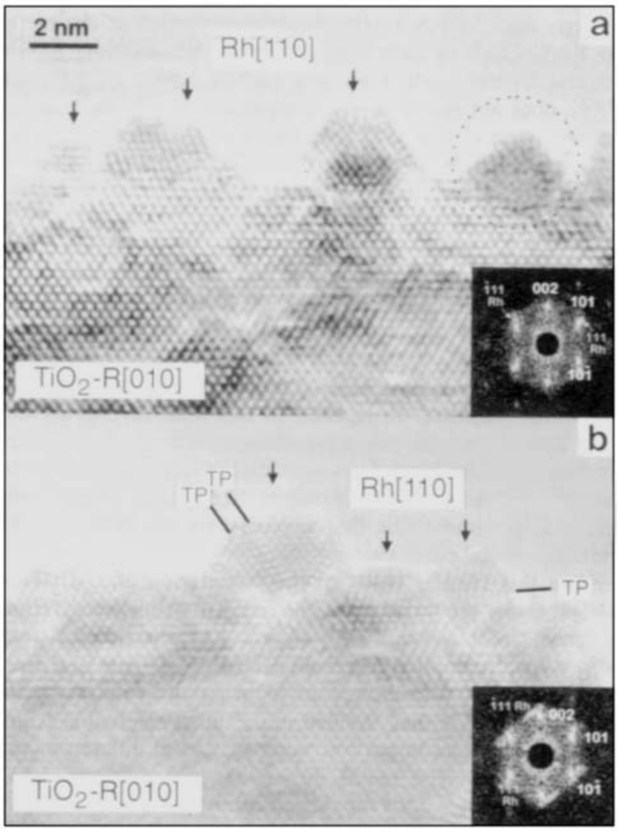

Fig. 14 Experimental HREM images recorded on the catalyst reduced at 773 K and further reoxidized at 673 K

Two other aspects worth commenting on in connection with the reoxidation treatment at 673 K are those concerning the effect of such a treatment on the metal particles. Upon low-temperature reduction (473 K) of the oxidized catalyst, Fig. 14 and 15, we may note that the metal particles do not recover the size distribution observed upon direct reduction of the precursor/support system at the same temperature. This

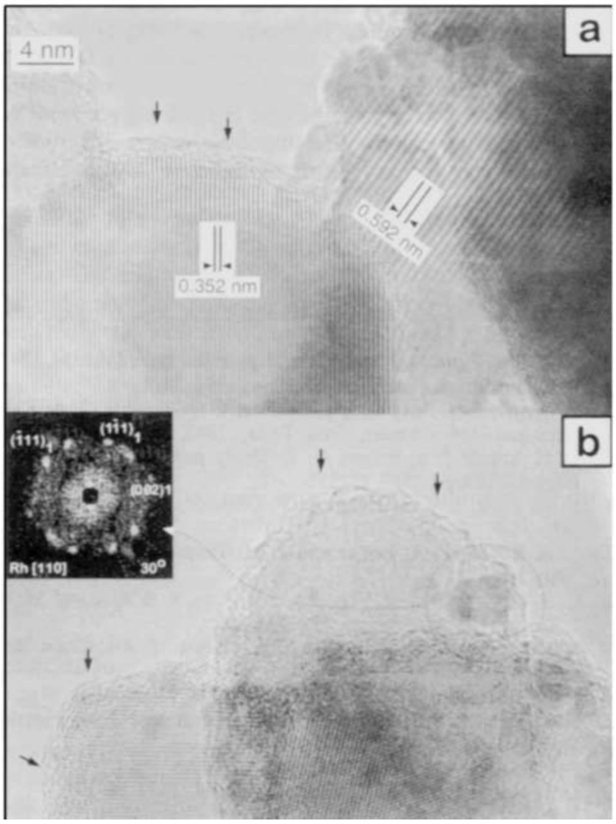

Fig. 15 Another region of the catalyst shown in Fig. 14. Note the large spacing fringes in (a) and the occurrence of twinned particles in (b).

suggests that there is no significant redispersion of the metal. On Rh/CeO$_2$,[4] we have made a similar observation, *i.e.* the reoxidation treatment, even at a slightly higher temperature, 773 K, does not induce metal redispersion. It was necessary to heat in flowing O$_2$ at 1173 K to find a significant modification of the particle size distribution.[4] Also worth noting is that the metal particles resulting from the low-temperature reduction of the reoxidized catalyst are often twinned. This twinning effect can be easily observed in the HREM images [twin planes (TP) marked in Fig. 14(b)] and, also, in the digital diffraction patterns like those shown as insets in Fig. 14(b) and 15(b). As already outlined, this can be due to the presence of twinned particles in the catalyst reduced at 773 K, but it could not be excluded that the reoxidation treatment could also have some influence. In relation to this idea, several authors have agreed on the polycrystalline nature of the oxidized rhodium particles formed upon oxidation of a dispersed metal phase.[4,64,65] Accordingly, it seems likely that a very mild reduction treatment like that applied here can lead to polycrystalline metal particles.

From this HREM study of the reoxidation of a Rh/TiO$_2$ catalyst under the SMSI state, the following conclusions could be drawn. In accordance with our results, the oxidizing treatment normally applied to recover the Rh/TiO$_2$ catalyst from the SMSI state, does not seem to bring the catalyst to the same condition as that reached upon direct reduction at low temperature. Quite important microstructural differences can be noted. First, the metal dispersions are different, being poorer in the case of the reoxidized catalyst. Secondly, the face development and defect content are also different from one catalyst to the other. Moreover, it does not seem that a full recovery from the metal decoration effects is achieved. All these observations might well explain the differences in chemisorptive and catalytic behaviour often reported in the literature.[13,40] In particular, differences should be expected in their behaviour for structure-sensitive catalytic reactions.[66]

This work has received financial support from the DGICYT (Project: PB92-0483), CICYT (Project: MAT95-1109E) and the Junta de Andalucía. We are very grateful to Dr. P. A. Stadelmann for his kind help in the installation and training with the EMS Software package. The HREM images reported here were obtained at the Electron Microscopy Facilities of the University of Cadiz. We thank Johnson Matthey for a loan of noble metals.

References

1 M. J. Yacamán and M. Avalos Borja, *Catal. Rev. Sci. Eng.*, 1992, **34**, 55.
2 A. K. Datye and D. J. Smith, *Catal. Rev. Sci. Eng.*, 1992, **34**, 129.
3 P. L. Gai-Boyes, *Catal. Rev. Sci. Eng.*, 1992, **34**, 1.
4 S. Bernal, F. J. Botana, J. J. Calvino, G. A. Cifredo, J. A. Pérez Omil and J. M. Pintado, *Catal. Today*, 1995, **28**, 219.
5 L. F. Allard, J. S. Brinen, F. P. Dayly and A. J. Garrat-Reed, *Ultramicroscopy*, 1987, **22**, 135.
6 K. C. Pratt, J. V. Sanders and V. Christov, *J. Catal.*, 1990, **124**, 416.
7 L. A. Bursill, E. A. Lodge and J. M. Thomas, *Nature (London)*, 1980, **286**, 111.
8 C. B. de Gruyter, J. P. Verduijn, J. Y. Koo, S. B. Rice and M. M. J. Treacy, *Ultramicroscopy*, 1990, **34**, 102.
9 S. J. Tauster, S. C. Fung and R. L. Garten, *J. Am. Chem. Soc.*, 1978, **100**, 170.
10 S. J. Tauster and S. C. Fung, *J. Catal.*, 1978, **55**, 29.
11 S. J. Tauster, S. C. Fung, R. T. K. Baker and J. A. Horsley, *Science*, 1981, **211**, 1121.
12 S. J. Tauster, *Acc. Chem. Res.*, 1987, **20**, 389.
13 G. L. Haller and D. E. Resasco, *Adv. Catal.*, 1989, **36**, 173.
14 J. P. Belzunegui, J. Sanz and J. M. Rojo, *J. Am. Chem. Soc.*, 1992, **114**, 6749.
15 D. Kalakkad, A. K. Datye and H. Robota, *Appl. Catal. B*, 1992, **1**, 191.
16 R. T. K. Baker, E. B. Prestidge and R. L. Garten, *J. Catal.*, 1979, **56**, 390.
17 R. T. K. Baker, E. B. Prestidge and R. L. Garten, *J. Catal.*, 1979, **59**, 293.
18 R. T. K. Baker, *J. Catal.*, 1980, **63**, 523.
19 R. T. K. Baker, E. B. Prestridge and L. L. Murrell, *J. Catal.*, 1983, **79**, 348.
20 R. T. K. Baker, J. J. Chludzinski and J. A. Dumesic, *J. Catal.*, 1985, **93**, 312.
21 A. J. Simoens, R. T. K. Baker, D. J. Dwyer, C. R. F. Lund and R. J. Madon, *J. Catal.*, 1984, **86**, 359.
22 J. A. Dumesic, S. A. Stevenson, R. D. Sherwood and R. T. K. Baker, *J. Catal.*, 1986, **99**, 79.
23 B. J. Tatarchuk, J. J. Chludzinski, R. D. Sherwood, J. A. Dumesic and R. T. K. Baker, *J. Catal.*, 1981, **70**, 433.
24 R. T. K. Baker, E. B. Prestidge and B. McVicker, *Catal.*, 1984, **89**, 422.
25 J. C. Vis, H. F. J. Van't Blik, T. Huizinga, J. van Grondelle and R. Prins, *J. Catal.*, 1985, **95**, 333.
26 S. Fuentes, A. Vázquez, R. Silva, J. G. Pérez Ramírez and M. J. Yacamán, *J. Catal.*, 1988, **111**, 353.
27 J. H. A. Martens, R. Prins, H. Zandbergen and D. C. Koningsberger, *J. Phys. Chem.*, 1988, **92**, 1903.
28 R. J. Fenoglio, G. M. Núñez and D. E. Resasco, *J. Catal.*, 1990, **121**, 77.
29 J. A. Cairns, J. E. E. Baglin, G. J. Clark and J. F. Ziegler, *J. Catal.*, 1983, **83**, 301.
30 M. J. Kelley, D. R. Short and D. G. Swartzfager, *J. Mol. Catal.*, 1983, **20**, 235.
31 H. R. Sadeghi and V. E. Henrich, *J. Catal.*, 1984, **87**, 279.
32 C. S. Ko and R. J. Gorte, *J. Catal.*, 1984, **90**, 59.
33 S. Takatani and Y. W. Chung, *J. Catal.*, 1984, **90**, 75.
34 D. N. Belton, Y. M. Sun and J. M. White, *J. Phys. Chem.*, 1984, **88**, 1690.
35 D. N. Belton, Y. M. Sun and J. M. White, *J. Phys. Chem.*, 1984, **88**, 5172.
36 D. J. Smith, R. W. Glaisher, P. Lu and M. R. McCartney, *Ultramicroscopy*, 1989, **29**, 123.
37 A. K. Singh, N. K. Pande and A. T. Bell, *J. Catal.*, 1985, **94**, 422.
38 A. D. Logan, E. J. Braunschweig, A. K. Datye and D. J. Smith, *Langmuir*, 1988, **4**, 827.
39 E. J. Braunschweig, A. D. Logan, A. K. Datye and D. J. Smith, *J. Catal.*, 1989, **118**, 227.
40 S. Bernal, J. J. Calvino, M. A. Cauqui, G. A. Cifredo, A. Jobacho and J. M. Rodríguez-Izquierdo, *Appl. Catal. A*, 1993, **99**, 1.
41 L. Wang, G. W. Qiao, H. Q. Ye, K. H. Kuo and Y. X. Chen, *Proceedings 9th. International Congress Catalysis (Calgari)*, ed. M. J. Philipps and M. Ternan, The Chem. Inst. Canada, Ottawa, 1988, vol. 3, p. 1253.
42 A. K. Datye, D. S. Kalakkad, M. H. Yao and D. J. Smith, *J. Catal.*, 1995, **155**, 148.
43 T. Komaya, A. T. Bell, Z. Weng-Sieh, R. Gronsky, F. Engelke, T. S. King and M. Pruski, *J. Catal.*, 1994, **149**, 142.
44 S. Bernal, F. J. Botana, J. J. Calvino, M. A. Cauqui, G. A. Cifredo, A. Jobacho, J. M. Pintado and J. M. Rodríguez-Izquierdo, *J. Phys. Chem.*, 1993, **97**, 4118.
45 S. Bernal, J. J. Calvino, G. A. Cifredo, A. Laachir, V. Perrichon and J. M. Herrmann, *Langmuir*, 1994, **10**, 717.
46 S. Bernal, F. J. Botana, R. García, F. Ramírez and J. M. Rodríguez-Izquierdo, *Appl. Catal.*, 1986, **21**, 379.
47 S. Bernal, F. J. Botana, R. García, F. Ramírez and J. M. Rodríguez-Izquierdo, *Appl. Catal.*, 1987, **31**, 267.
48 S. Bernal, F. J. Botana, R. García, F. Ramírez and J. M. Rodríguez-Izquierdo, *J. Chem. Soc., Faraday Trans. 1*, 1987, **83**, 2279.
49 S. Bernal, F. J. Botana, R. García, F. Ramírez and J. M. Rodríguez-Izquierdo, *J. Mater. Sci.*, 1987, **22**, 3793.
50 R. Kieffer, A. Kiennemann, M. Rodríguez, S. Bernal and J. M. Rodríguez-Izquierdo, *Appl. Catal.*, 1988, **42**, 77.
51 S. Bernal, F. J. Botana, R. García, Z. Kang, M. L. López, M. Pan, F. Ramírez and J. M. Rodríguez-Izquierdo, *Catal. Today*, 1988, **2**, 653.
52 S. Bernal, F. J. Botana, R. García and J. M. Rodríguez-Izquierdo, *Stud. Surf. Sci. Catal.*, 1989, **48**, 123.
53 S. Bernal, F. J. Botana, G. A. Cifredo, J. J. Calvino, R. García and J. M. Rodríguez-Izquierdo, *Ultramicroscopy*, 1990, **34**, 60.
54 S. Bernal, G. A. Cifredo, J. J. Calvino, J. M. Rodríguez-Izquierdo, V. Perrichon and A. Laachir, *J. Chem. Soc., Chem. Commun.*, 1992, 460.
55 S. Bernal, G. A. Cifredo, J. J. Calvino, J. M. Rodríguez-Izquierdo, V. Perrichon and A. Laachir, *J. Catal.*, 1992, **137**, 1.

56 S. Bernal, J. J. Calvino, G. A. Cifredo, J. M. Gatica, J. A. Pérez Omil, A. Laachir and V. Perrichon, *Stud. Surf. Sci. Catal.*, 1995, **96**, 419.

57 C. Binet, A. Jadi, J. C. Lavalley and M. Bounet-Kizling, *J. Chem. Soc., Faraday Trans.*, 1992, **88**, 2079.

58 R. P. Underwood and A. T. Bell, *Appl. Catal.*, 1987, **34**, 289.

59 J. P. Belzunegui, J. M. Rojo and J. Sanz, *J. Phys. Chem.*, 1991, **95**, 3463.

60 M. Pan, J. M. Cowley and R. García, *Micron. Microsc. Acta*, 1987, **18**, 165.

61 G. J. Wood, L. A. Bursill and D. J. Smith, *J. Microscopy*, 1983, **129**, 263.

62 B. G. Hyde and S. Andersson, *Inorganic Crystal Structures*, Wiley Interscience, New York, 1989.

63 J. C. Conesa and J. Soria, *J. Phys. Chem.*, 1982, **86**, 1392.

64 A. D. Logan, E. J. Braunschweig, A. K. Datye and D. J. Smith, *Ultramicroscopy*, 1989, **31**, 132.

65 S. Chakraborti, A. K. Datye and N. J. Long, *J. Catal.*, 1987, **108**, 444.

66 A. D. Logan, K. Sharoudi and A. K. Datye, *J. Phys. Chem.*, 1991, **95**, 5568.

Paper 6/00311G; *Received* 15*th January*, 1996